

## Report

# Anchorage of Plant RanGAP to the Nuclear Envelope Involves Novel Nuclear-Pore-Associated Proteins

Xianfeng Morgan Xu,<sup>1</sup> Tea Meulia,<sup>2</sup> and Iris Meier<sup>1,\*</sup><sup>1</sup> Plant Biotechnology Center and Department of Plant Cellular and Molecular BiologyThe Ohio State University  
Columbus, Ohio 43210<sup>2</sup> Molecular and Cellular Imaging CenterOhio Agricultural Research and Development Center  
The Ohio State University  
Wooster, Ohio 44691

## Summary

The Ran GTPase controls multiple cellular processes including nucleocytoplasmic transport, spindle assembly, and nuclear envelope (NE) formation [1–4]. Its roles are accomplished by the asymmetric distribution of RanGTP and RanGDP enabled by the specific locations of the Ran GTPase-activating protein RanGAP and the nucleotide exchange factor RCC1 [5–8]. Mammalian RanGAP1 targeting to the NE and kinetochores requires interaction of its sumoylated C-terminal domain with the nucleoporin Nup358/RanBP2 [9–14]. In contrast, *Arabidopsis* RanGAP1 is associated with the NE and cell plate, mediated by an N-terminal, plant-specific WPP domain [15–18]. In the absence of RanBP2 in plants, the mechanism for spatially sequestering plant RanGAP is unknown. Here, *Arabidopsis* WPP-domain interacting proteins (WIPs) that interact with RanGAP1 in vivo and colocalize with RanGAP1 at the NE and cell plate were identified. Immunogold labeling indicates that WIP1 is associated with the outer NE. In a *wip1-1/wip2-1/wip3-1* triple mutant, RanGAP1 is dislocated from the NE in undifferentiated root-tip cells, whereas NE targeting in differentiated root cells and targeting to the cell plate remain intact. We propose that WIPs are novel plant nucleoporins involved in RanGAP1 NE anchoring in specific cell types. Our data support a separate evolution of RanGAP targeting mechanisms in different kingdoms.

## Results and Discussion

### Identification of an *Arabidopsis* RanGAP-Binding Protein Family

A yeast two-hybrid screen was performed to identify proteins that interact with *Arabidopsis* RanGAP1. WPP-domain Interacting Protein 1 (WIP1, At4g26450) was found to bind full-length RanGAP1 as well as the WPP domain, but not RanGAP1 without the WPP domain (Figure 1C). WIP1 is a previously undescribed protein with a predicted C-terminal transmembrane domain and an adjacent coiled-coil domain (Figure 1A). Coimmunoprecipitation (co-IP) from either RanGAP1-GFP or GFP-WIP1 transgenic *Arabidopsis* plants

confirmed the interaction between RanGAP1 and WIP1 in vivo (Figure 1B).

WIP1-like proteins were identified from several other higher plant species (Figure S2B in the Supplemental Data available online). In *Arabidopsis*, At5g56210 (WIP2) and At3g13360 (WIP3) encode the most closely related proteins (Table 1). All WIP-like proteins shared similar domain structures, including an NLS (Figure 1A and Figure S3), the coiled-coil domain, and the putative transmembrane domain. Available cDNA sequences indicate that two WIP2 alternative splicing forms exist. WIP2a contained all the domains conserved in the whole family, whereas WIP2b lacked the N-terminal 220 amino acids including the NLS (see Figure 3A). No WIP-like proteins were identifiable from nonplant species.

To test WIP2a and WIP3 for interaction with RanGAP1, map the interaction domain of WIP1, and test the binding of WIP family members to other *Arabidopsis* WPP-domain proteins, we assayed yeast two-hybrid interactions. Two WIP1 fragments were generated, representing the N-terminal 312 amino acids (WIP1N) and the coiled-coil domain (WIP1cc) (amino acids 313–459). Two previously described fragments of RanGAP1 were tested, RanGAP1ΔC (amino acids 1–119, representing the WPP domain) and RanGAP1ΔN (amino acids 120–535, RanGAP1 without the WPP domain) [15, 16]. *Arabidopsis* expresses five WPP-domain proteins. In addition to RanGAP1, these are the second RanGAP (RanGAP2) and three short proteins with similarity to the N terminus of RanGAP, WPP1, WPP2, and WPP3. WPP1 and WPP2 associate with the NE, whereas WPP3 is cytoplasmic and nuclear. Knockdown mutants of the WPP gene family have root growth defects [19].

The RanGAP1 WPP domain (BD-RanGAP1ΔC) and the WIP1 coiled-coil domain (AD-WIP1cc) are necessary and sufficient for RanGAP1-WIP1 interaction (Figure 1C). WIP2a and WIP3 bind the WPP domain of RanGAP1 but not full-length RanGAP1. RanGAP2 binds WIP1 and WIP2a but not WIP3, and the WIP1 coiled-coil domain is necessary and sufficient for the interaction with RanGAP2. WPP1 and WPP2 bind all three WIP full-length proteins and the WIP1 coiled-coil domain, whereas WPP3 does not bind WIP family members. WIP2a does homodimerize as well as heterodimerize with WIP1, but not with WIP3. The WIP1 coiled-coil domain is necessary and sufficient for heterodimerization with WIP2. WIP3 neither homodimerizes nor heterodimerizes with WIP1 or WIP2a.

### Subcellular Localization of the WIP Protein Family and the WIP-RanGAP Interaction

To test whether the WIP family members are located at the nuclear envelope, we visualized N-terminal GFP fusion proteins in transgenic *Arabidopsis* roots. GFP-WIP1, GFP-WIP2a, and GFP-WIP3 clearly associated with the NE (Figure 2A). Colocalization of WIP1 and RanGAP1 at the NE was confirmed in GFP-WIP1 transgenic plants by double immunolabeling with a mouse

\*Correspondence: [meier.56@osu.edu](mailto:meier.56@osu.edu)

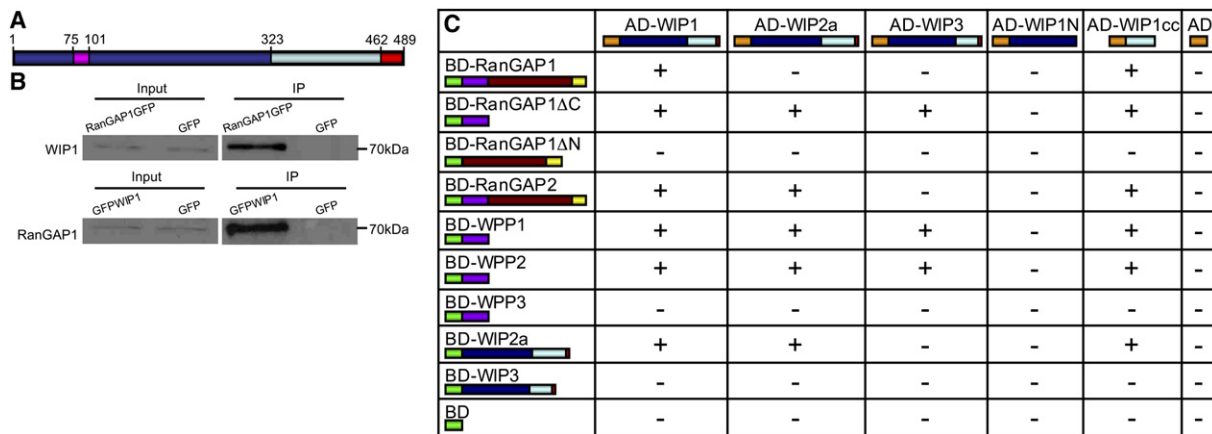


Figure 1. The Coiled-Coil Domain of WIP1 Interacts with the WPP Domain of RanGAP

(A) Domain structure of WIP1. WIP1 has an extended coiled-coil domain (sky blue) and a single, C-terminal transmembrane domain (red). A bipartite NLS is the only recognizable motif (pink; see Figure S3) amino terminal (dark blue) of the coiled-coil domain. Numbers above the bar indicate amino acid positions.

(B) WIP1 and RanGAP1 are in the same complex in vivo, shown by co-IP. Samples immunoprecipitated (IPed) with the GFP antibody from RanGAP1-GFP and GFP expressing lines were probed with WIP1 antibody (top). Samples IPed with the GFP antibody from GFP-WIP1 and GFP lines were probed with RanGAP1 antibody (bottom). Inputs are shown on the left.

(C) Interaction between the WIP1 family and *Arabidopsis* WPP-domain-containing proteins in yeast two-hybrid assays. Fusion proteins are schematically shown below the construct names. AD, GAL4 activation domain; BD, GAL4 DNA binding domain. Plus (+), positive interaction; (-), no interaction. (WIP1, WIP1N, and WIP1cc self-activate and were only tested as AD fusions.)

GFP antibody and rabbit RanGAP1 antibody (Figure 2B, upper panel). Double labeling with a nuclear pore marker (QE5, recognizing Nup214, Nup153, and p62 in mammals) [20] showed a strong correlation between the GFP and QE5 staining (Figure 2B, lower panel).

In yeast two-hybrid assays WIP2a and WIP3 interacted with the WPP domain of RanGAP1 but not full-length RanGAP1 (Figure 1C). To test protein-protein interactions in planta, we employed bimolecular fluorescence complementation (BiFC) [21, 22]. Figure 2C shows that in planta, all three WIP family members are capable of interacting with RanGAP1 and with WPP1 at the NE.

Like animal cells, plant cells undergo open mitosis with NE breakdown during prophase and reassembly during telophase [23]. However, whereas animal cells divide by furrow ingression and scission, plant cytokinesis involves the assembly of new plasma membrane and cell wall (called the cell plate) via the phragmoplast, a microtubule-based structure possibly analogous to the spindle midzone or midbody [24]. *Arabidopsis* RanGAP1 was shown to associate with the nascent cell plate

during cytokinesis, suggesting an additional role for the Ran cycle during plant-cell division [16]. Here, we show that GFP-WIP1 and GFP-WIP2a colocalize with RanGAP1 at the cell plate in dividing root-tip cells, whereas GFP-WIP3 appears at the reforming nuclei but not the cell plate (Figure 2D).

The fact that both RanGAP1 and the short WPP-domain protein WPP1 are targeted to the NE during interphase and to the cell plate during cytokinesis has suggested an unrecognized mechanistic connection between these two membrane-rearrangement events [16, 19]. The fact that WIP1 and WIP2a, two putative transmembrane NPC proteins (see below), also reside on the cell plate strengthens the idea that the two membrane compartments share some identity.

### Ultrastructural Analyses of WIP1 and RanGAP1 Localization at the NE

Mammalian RanGAP1 and its NE anchor RanBP2/Nup358 have been mapped ultrastructurally at the cytoplasmic filaments of the NPC [11, 12, 25], suggesting that plant RanGAP might also be at the cytoplasmic side of the NE and enriched around the NPC [18, 26]. A series of Z stack confocal images were taken, spanning half of the nucleus in GFP-WIP1 expressing root callus cells. When a 3D maximal projection was constructed, the GFP signal appeared in a dotted pattern (Figure 2E, left panel), which closely resembled the NPCs, illustrated by scanning electron microscopy of *Arabidopsis* root callus nuclei (Figure 2E, middle and right panels).

Subcellular localization of plant RanGAP1 and WIP1 was further investigated with transmission electron microscopy (TEM) after embedding immunogold labeling. The gold labeling is consistent with RanGAP1 accumulating at the cytoplasmic side of the NE and with the fact that most of RanGAP1 is in association with nuclear

Table 1. Percent Identity and Similarity on Amino Acid Sequence Level among WIP1 Family Members and WIP-like Proteins

	WIP2a	WIP3	Rice BAD08716	Rice BAD46344	Wheat CAJ19339
WIP1	40 (51)	31 (47)	24 (43)	24 (43)	24 (40)
WIP2a	-	31 (45)	23 (37)	23 (42)	25 (41)
WIP3	-	-	21 (37)	ND	26 (41)
Rice BAD08716	-	-	-	42 (56)	41 (55)
Rice BAD46344	-	-	-	-	61 (71)

Percent similarities are shown in parentheses. Rice (*Oryza sativa*). Wheat (*Triticum aestivum*). ND, no similarity detected.

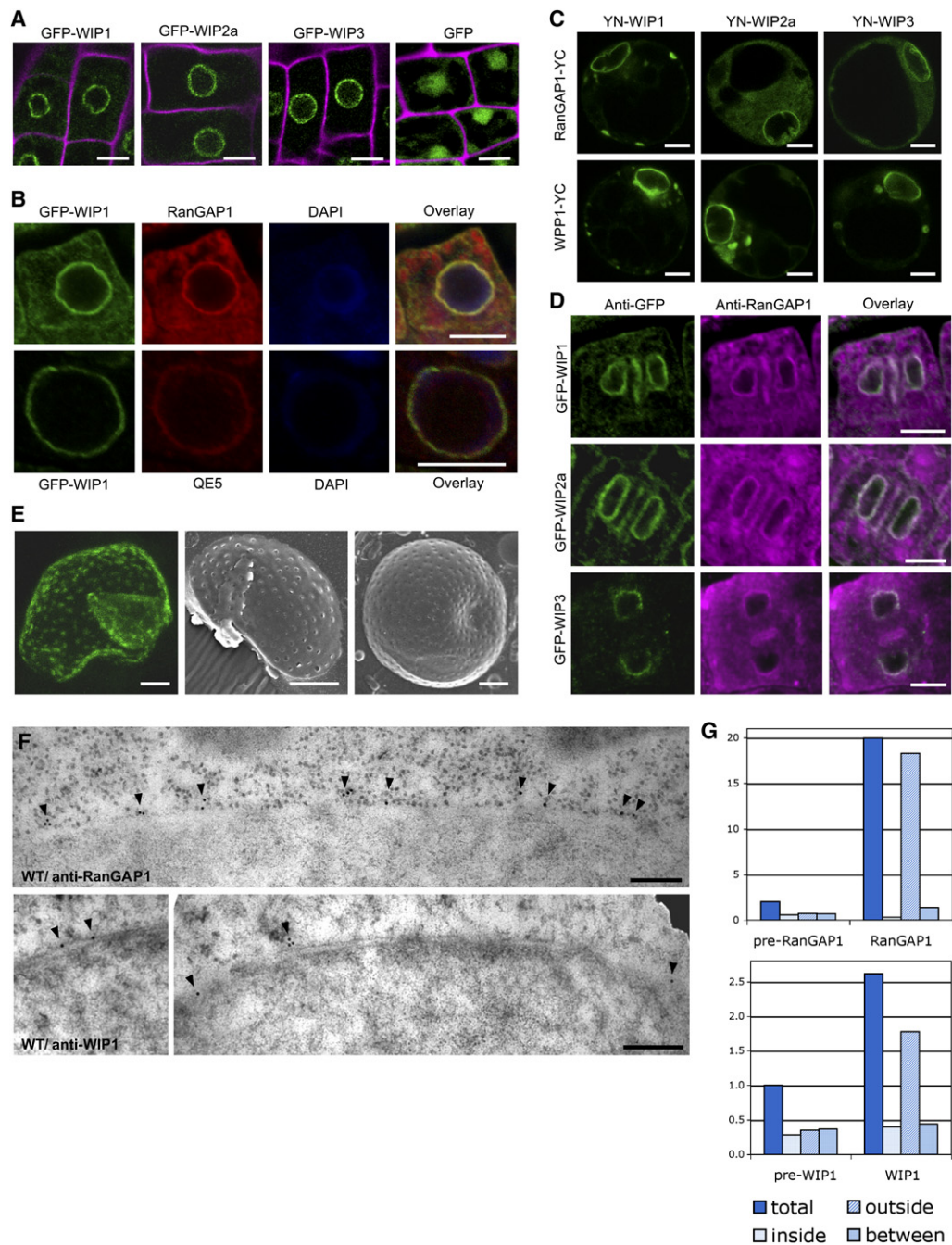


**Figure 2. WIP1 and RanGAP1 Interact at the Outer NE, Most Likely at the Cytoplasmic Side of the NPC**

(A) GFP-WIP1, GFP-WIP2a, and GFP-WIP3 are targeted to the NE in *Arabidopsis* root-tip cells, whereas free GFP is distributed throughout the nucleus and cytoplasm. Confocal images were taken from transgenic lines expressing 35S promoter-controlled fusion proteins with cell walls stained with propidium iodide (magenta).

(B) Double immunofluorescence of GFP-WIP1 and RanGAP1 or the NPC marker QE5 in *Arabidopsis* root-tip cells, with DNA counterstained with DAPI.

(C) RanGAP1 and WPP1 interact with WIP1, WIP2a, and WIP3 at the NE in *Nicotiana benthamiana* protoplasts, as shown by BiFC. YN, N-terminal domain of YFP; YC, C-terminal domain of YFP. None of the constructs showed fluorescence when transfected into protoplasts alone or when cotransfected with an empty YN or YC vector (data not shown). The position of the nucleus was judged by bright-field images (not shown).

(D) GFP-WIP1 and GFP-WIP2a, but not GFP-WIP3 (green), colocalize with RanGAP1 (magenta) at the cell plate, revealed by immunofluorescence in transgenic *Arabidopsis* root-tip cells. GFP-WIP3 is targeted to the daughter NE but not to the cell plate during cytokinesis. Scale bars in (A)–(D) represent 10  $\mu$ m.

(E) Three-dimensional maximal projection of confocal images spanning half of the nucleus from root callus cells expressing GFP-WIP1 (left panel), and nuclei with nuclear pores from *Arabidopsis* root callus cells visualized by scanning electron microscopy (middle and right panels). The density of dotted signal from GFP-WIP1 is similar to the density of NPCs. Scale bars represent 1  $\mu$ m.

(F) Micrographs showing representative images of postembedding immunogold labeling of RanGAP1 (top panel, WT/anti-RanGAP1) and WIP1 (bottom panels, WT/anti-WIP1) in wild-type *Arabidopsis* root callus tissues. Scale bars represent 100 nm.

(G) Graphical representation of the numbers shown in Table 2.



Table 2. Quantification of the Immunogold Labeling for RanGAP1 and WIP1

Antibody	Gold Part./10 $\mu\text{m}$ Total	Gold Part./10 $\mu\text{m}$ Inside	Gold Part./10 $\mu\text{m}$ Outside	Gold Part./10 $\mu\text{m}$ Between	Total Nucl. Perimeter ( $\mu\text{m}$ )	Nb Nuclei Counted
pre-RanGAP1	2.02	0.58	0.74	0.70	954.4	74
anti-RanGAP1	19.97	0.31	18.28	1.38	763.1	52
pre-WIP1	1.00	0.28	0.35	0.37	1198.4	92
anti-WIP1	2.62	0.40	1.78	0.44	748.9	54

"Nb Gold Part./10  $\mu\text{m}$ " stands for the number of gold particles counted per 10  $\mu\text{m}$  of the NE. The distribution of the gold particles was shown for inside of the NE, outside of the NE, and between the double membranes. "Total Nucl. Perimeter" stands for the total length of the nuclear perimeter (envelope) measured for each specimen with ImageJ. "Nb Nuclei Counted" stands for the number of nuclei counted for each specimen.

pores (Figure 2F, top panel). The WIP1 antibody gave a lower amount of signal compared to RanGAP1, however the WIP1 antibody signal was still 2.6-fold above the preimmune background (Figure 2G and Table 2; for background quantification, see Supplemental Experimental Procedures). Gold particles were detected at the outer surface of the NE, mostly in association with nuclear pores (Figure 2F, lower panels). Taken together, both the fluorescence microscopy and TEM data support the idea that WIP1 is an outer NE protein, most likely to be located at the nuclear pore.

WIP1 is the first available plant protein to track the fate of the plant NE during cell cycle. We therefore followed the dynamics of GFP-WIP1 during mitosis and cytokinesis (Figure S1). Our data show that similar to the animal NE [27], plant NE reassembly commences in anaphase and appears complete concomitant with early cell-plate formation.

#### Domain Requirement for the Subcellular Targeting of WIP1

If WIP1 is an anchor for plant RanGAP at membrane systems, we would predict that its own targeting to the NE and cell plate is independent of the RanGAP1-binding domain and is likely to be dependent on the transmembrane domain. To determine which domain is responsible for targeting WIP1 to the NE and cell plate, we fused different deletion constructs to GFP and visualized them in root cells of transgenic *Arabidopsis* (Figure S2). The data show that WIP1 is indeed targeted to the NE and cell plate via its C terminus, probably by direct membrane association, consistent with the features postulated for a RanGAP anchor.

#### Role of the WIP Family in RanGAP Anchoring

Transfer-DNA (T-DNA) insertion lines in each WIP locus were identified (Figure 3A). In *wip1-1*, neither WIP1 RNA nor WIP1 protein could be detected, consistent with a knockout mutation, and in *wip3-1*, no WIP3 RNA could be detected. Because of the two alternative splicing variants of WIP2, the insertion in *wip2-1* is located in the first exon of WIP2a and the first intron of WIP2b. This line was a knockout for WIP2a and a severe knockdown for WIP2b, on the basis of RNA level (Figure 3B). Individual homozygous insertion lines were tested by immunofluorescence for RanGAP1 localization, and no difference from wild-type plants was found (data not shown). Lines were therefore crossed to obtain all double-mutant combinations and a triple mutant. No difference in RanGAP1 localization was found in the double mutants (data not shown).

Strikingly, however, both endogenous RanGAP1 and RanGAP1-GFP were absent from the NE in root-tip cells of the *wip1-1/wip2-1/wip3-1* triple-mutant line (Figures 3C and 3D). Although RanGAP1 NE accumulation was entirely lost in root-tip cells (including both the meristem and elongation zone), the association was unchanged in cells from the root differentiation zone (defined by the appearance of root hairs [28]). QE5 decoration of the NE was not altered in *wip1-1/wip2-1/wip3-1*, indicating the absence of gross alterations in NPC or NE assembly. Figure 3D shows that, like RanGAP1-GFP, a GFP fusion protein of the N-terminal RanGAP1 WPP domain also lost association with the NE in root tips of *wip1-1/wip2-1/wip3-1* triple mutants (note that this fusion protein also enters the nucleus because of its small size), indicating that loss of NE targeting reflects loss of WPP-domain binding. Again, NE association was not lost in differentiated cells. Similarly, in *wip1-1/wip2-1/wip3-1* triple mutants, RanGAP2 lost its concentration on the NE in the root-tip zone but not in differentiated cells, shown by a GFP fusion protein (Figure 3D). As a control, RanGAP1(AAP)-GFP with the WPP motif mutated to AAP lost the association with the NE in all cell types (Figure 3D).

To confirm that the lack of RanGAP1 NE association in *wip1-1/wip2-1/wip3-1* was because of the absence of the three proteins and that WIP1, WIP2a, and WIP3 function redundantly in anchoring RanGAP1 to the root-tip NE, we separately retransformed *wip1-1/wip2-1/wip3-1* with the GFP fusions of each protein. Figure 4A shows that in the *wip1-1/wip2-1/wip3-1* mutant expressing any GFP-WIP fusion protein, RanGAP1 NE association was re-established in root-tip cells. This clearly demonstrates that the GFP fusion proteins are functional and that any single WIP paralog is sufficient for RanGAP1 NE targeting in root-tip cells. In addition, consistent with the results that the coiled-coil domain of WIP1 interacts with RanGAP and the N-terminal domain is dispensable for the targeting of WIP1 to the NE, GFP-WIP1 $\Delta\text{N}$  is sufficient to recruit RanGAP1 and cause RanGAP1 accumulation around the NE in the triple mutant (Figure 4A).

The *wip1-1/wip2-1/wip3-1* mutant plants had no observable defect in growth or development under standard laboratory conditions and no change in auxin sensitivity was observed in a standard root-elongation assay (data not shown; see [29]).

Finally, we investigated the mitotic localization pattern of RanGAP1 in the *wip1-1/wip2-1/wip3-1* root meristem. Figure 4B shows that RanGAP1 association with the cell plate was indistinguishable from wild-type

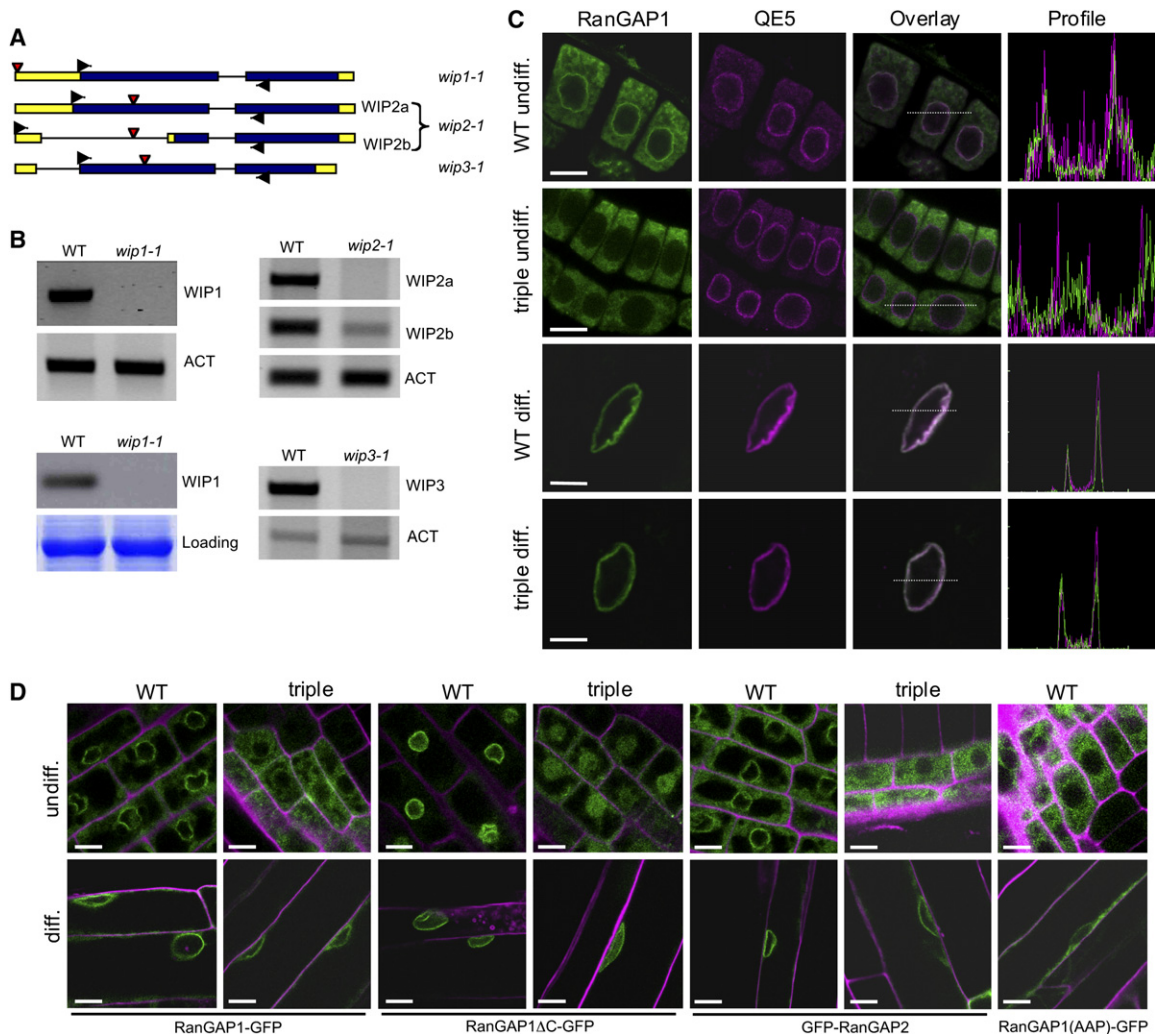


**Figure 3.** In the *wip1-1/wip2-1/wip3-1* Triple Mutant, RanGAP1 Is Dislocated from the NE in Undifferentiated Root Cells, whereas NE Targeting in Differentiated Cells Is Not Affected

(A) Schematic representation of T-DNA insertions in *wip1-1*, *wip2-1*, and *wip3-1*. Colored boxes stand for the following: blue boxes, open reading frames; black lines, introns; yellow boxes, untranslated regions; red vertical arrowheads, T-DNA insertion sites; and black horizontal arrowheads, sites of RT-PCR primers.

(B) The top-left panel shows *wip1-1* RT-PCR analysis; the bottom-left panel shows *wip1-1* immunoblot analysis with the WIP1 antibody. The top-right panel shows *wip2-1* RT-PCR analysis; the bottom right panel shows *wip3-1* RT-PCR analysis. ACT, Actin 2; "Loading," Coomassie brilliant blue staining of a replica gel.

(C) Immunofluorescence localization of RanGAP1 and the NE marker QE5 in the wild-type and *wip1-1/wip2-1/wip3-1* triple mutant. "Undiff." stands for undifferentiated root-tip cells (meristem and elongation zone); "diff." stands for differentiated root cells. "Profile" stands for the fluorescence-intensity profile of dotted lines in overlay images. In all cases except the undifferentiated cells from the triple mutant, peaks of green signal (RanGAP1) correlate with peaks of magenta signal (QE5) representing the NE.

(D) Root cells of transgenic wild-type and *wip1-1/wip2-1/wip3-1* lines expressing GFP fusions of RanGAP1, RanGAP1 $\Delta$ C (see Figure 1C), RanGAP2, and RanGAP1(AAP)-GFP carrying a WPP to AAP mutation in the RanGAP1 targeting domain [15], thereby leading to loss of NE targeting in all cell types. Cell walls were counterstained with propidium iodide (magenta). All scale bars represent 10  $\mu$ m.

plants at both early and late stages of cell-plate formation. This suggests that unlike NE association, concentration of RanGAP1 at the cell plate does not depend on the WIP family.

Our previous data suggested that plant and animal RanGAP have separately acquired kingdom-specific protein interaction domains [15, 16]. We therefore proposed that they have adapted interactions with different proteins for their interphase and mitotic subcellular anchoring that are required to establish the functional Ran gradients of the respective organism. In support of this hypothesis, we have identified here a family of

plant-specific NE anchors for plant RanGAP. Interestingly, we have also uncovered cell-type-specific differences in plant RanGAP NE anchoring. All available studies on animal RanGAP NE anchoring were performed at the single-cell level and thus did not address potential differences between tissues or developmental stages [9–14]. It is therefore currently unclear whether tissue-specific differences in RanGAP targeting are unique to plants or whether such differences (and additional anchoring activities besides RanBP2) also exist in animals. Our data indicate that whereas at the *Arabidopsis* root tip anchoring of RanGAP at the NE depends on

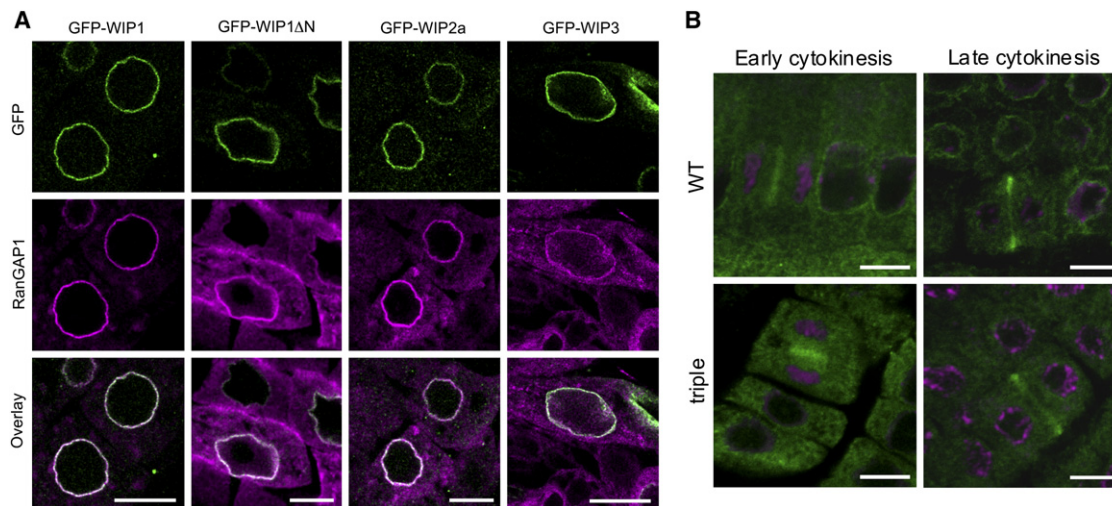


**Figure 4. RanGAP Targeting to the NE, but Not the Cell Plate, Depends on the WIP Family**

(A) GFP-WIP1, GFP-WIP1 $\Delta$ N, GFP-WIP2a, and GFP-WIP3 rescue RanGAP1 NE targeting in undifferentiated *wip1-1/wip2-1/wip3-1* root-tip cells. GFP (green) and RanGAP1 (magenta) antibodies were used for immunofluorescence in *wip1-1/wip2-1/wip3-1* mutants stably expressing the corresponding GFP fusion protein driven by the 35S promoter.

(B) RanGAP1 (green) is concentrated at the cell plate in *wip1-1/wip2-1/wip3-1* mutants during early and late cytokinesis, tested by immunofluorescence. DNA was visualized by SYTOX Orange (magenta). All scale bars represent 10  $\mu$ m.

the WIP family, in differentiated root cells and in hypocotyl cells, additional players are likely to be involved. It is possible that the level of redundancy of RanGAP NE anchoring differs in different cell types or that an unknown protein (or proteins) takes over the role of the WIP family in different tissues. The dependence of RanGAP anchoring on the WIP family at the root tip is consistent with the high expression of all three WIP genes in this region (Figure S4).

On the basis of the localization pattern of WIP1 revealed by the fluorescent and TEM immunolocalizations, the presence of its C-terminal transmembrane domain necessary and sufficient for NE localization, and its functional similarity with Nup358/RanBP2, we propose that WIP1 might be a novel, plant-specific nucleoporin. Although many nucleoporins share recognizable homologs in all extant eukaryotic lineages, kingdom-specific NE anchoring nucleoporins do exist in fungi and animals, and this indicates that they are a relatively recent innovation [30, 31]. This is consistent with WIP family members representing plant-specific anchoring nucleoporins.

Mammalian and plant RanGAP is concentrated at the NE, whereas yeast RanGAP is not. This has led to the question of what the function of this local concentration in some organisms might be. At least for the *Arabidopsis* root tip, we can conclude that RanGAP association with the NE is dispensable because normal growth and development (and therefore by inference nuclear import and export) are unchanged in a *wip1-1/wip2-1/wip3-1* triple mutant. It is possible that the advantage of RanGAP at the NE is greater in larger cells than in smaller cells because a large cytoplasm otherwise “dilutes out” RanGAP. This might explain why our triple mutant shows no obvious growth or development defects, because RanGAP delocalization occurs only in the small, undifferentiated cells of the root tip.

#### Supplemental Data

Experimental Procedures and four figures are available at <http://www.current-biology.com/cgi/content/full/17/13/1157/DC1/>.

#### Acknowledgments

We thank SIGnAL and the Arabidopsis Biological Resource Center for providing the sequence-indexed *Arabidopsis* T-DNA insertion mutants. We are in debt to Kelly Threm for help with the yeast two-hybrid screen. We are grateful to Qiao Zhao, Dr. Jelena Brkljacic, Dr. Annkatrin Rose, and members of the Meier lab for fruitful discussions, Dr. Shalaka Patel for the RanGAP(AAP)-GFP seeds, and Qiao Zhao for the pENTR/D-TOPO-RanGAP2 vector. We thank Dr. Biao Ding for generous user time of his confocal microscope and Dr. Kent McDonald, Dr. Elaine Humphrey, Dr. Andres Kaech, and the staff of the BI-Imaging at the University of British Columbia for their help and access to the equipment for the cryoelectron microscopy. We also thank Andrea Kaszas for technical help with the transmission electron microscopy. Thanks to Chao (Sylvia) He for general lab assistance and critical reading of the manuscript. Financial support from the National Science Foundation to I.M. is greatly acknowledged.

Received: February 17, 2007

Revised: May 11, 2007

Accepted: May 30, 2007

Published online: June 28, 2007

#### References

1. Amaoutov, A., and Dasso, M. (2003). The Ran GTPase regulates kinetochore function. *Dev. Cell* 5, 99–111.
2. Dasso, M. (2002). The Ran GTPase: Theme and variations. *Curr. Biol.* 12, R502–R508.
3. Hetzer, M., Gruss, O.J., and Mattaj, I.W. (2002). The Ran GTPase as a marker of chromosome position in spindle formation and nuclear envelope assembly. *Nat. Cell Biol.* 4, E177–E184.
4. Quimby, B.B., and Dasso, M. (2003). The small GTPase Ran: Interpreting the signs. *Curr. Opin. Cell Biol.* 15, 338–344.
5. Bischoff, F.R., Klebe, C., Kretschmer, J., Wittinghofer, A., and Ponstingl, H. (1994). RanGAP1 induces GTPase activity of nuclear Ras-related Ran. *Proc. Natl. Acad. Sci. USA* 91, 2587–2591.

6. Bischoff, F.R., and Ponstingl, H. (1991). Catalysis of guanine nucleotide exchange on Ran by the mitotic regulator RCC1. *Nature* 354, 80–82.
7. Kalab, P., Weis, K., and Heald, R. (2002). Visualization of a Ran-GTP gradient in interphase and mitotic *Xenopus* cell extracts. *Science* 295, 2452–2456.
8. Izaurralde, E., Kutay, U., von Kobbe, C., Mattaj, I.W., and Gorlich, D. (1997). The asymmetric distribution of the constituents of the Ran system is essential for transport into and out of the nucleus. *EMBO J.* 16, 6535–6547.
9. Matunis, M.J., Wu, J., and Blobel, G. (1998). SUMO-1 modification and its role in targeting the Ran GTPase-activating protein, RanGAP1, to the nuclear pore complex. *J. Cell Biol.* 140, 499–509.
10. Mahajan, R., Gerace, L., and Melchior, F. (1998). Molecular characterization of the SUMO-1 modification of RanGAP1 and its role in nuclear envelope association. *J. Cell Biol.* 140, 259–270.
11. Mahajan, R., Delphin, C., Guan, T., Gerace, L., and Melchior, F. (1997). A small ubiquitin-related polypeptide involved in targeting RanGAP1 to nuclear pore complex protein RanBP2. *Cell* 88, 97–107.
12. Matunis, M.J., Coutavas, E., and Blobel, G. (1996). A novel ubiquitin-like modification modulates the partitioning of the Ran-GTPase-activating protein RanGAP1 between the cytosol and the nuclear pore complex. *J. Cell Biol.* 135, 1457–1470.
13. Joseph, J., Liu, S.-T., Jablonski, S.A., Yen, T.J., and Dasso, M. (2004). The RanGAP1-RanBP2 complex is essential for microtubule-kinetochore interactions in vivo. *Curr. Biol.* 14, 1–20.
14. Joseph, J., Tan, S.H., Karpova, T.S., McNally, J.G., and Dasso, M. (2002). SUMO-1 targets RanGAP1 to kinetochores and mitotic spindles. *J. Cell Biol.* 156, 595–602.
15. Rose, A., and Meier, I. (2001). A domain unique to plant RanGAP is responsible for its targeting to the plant nuclear rim. *Proc. Natl. Acad. Sci. USA* 98, 15377–15382.
16. Jeong, S., Rose, A., Joseph, J., Dasso, M., and Meier, I. (2005). Plant-specific mitotic targeting of RanGAP requires a functional WPP domain. *Plant J.* 42, 270–282.
17. Meier, I. (2000). A novel link between ran signal transduction and nuclear envelope proteins in plants. *Plant Physiol.* 124, 1507–1510.
18. Pay, A., Resch, K., Frohnmeyer, H., Fejes, E., Nagy, F., and Nick, P. (2002). Plant RanGAPs are localized at the nuclear envelope in interphase and associated with microtubules in mitotic cells. *Plant J.* 30, 699–709.
19. Patel, S., Rose, A., Meulia, T., Dixit, R., Cyr, R.J., and Meier, I. (2004). Arabidopsis WPP-domain proteins are developmentally associated with the nuclear envelope and promote cell division. *Plant Cell* 16, 3260–3273.
20. Pante, N., Bastos, R., McMorro, I., Burke, B., and Aebi, U. (1994). Interactions and three-dimensional localization of a group of nuclear pore complex proteins. *J. Cell Biol.* 126, 603–617.
21. Hu, C.D., Chinenov, Y., and Kerppola, T.K. (2002). Visualization of interactions among bZIP and Rel family proteins in living cells using bimolecular fluorescence complementation. *Mol. Cell* 9, 789–798.
22. Bracha-Drori, K., Shichrur, K., Katz, A., Oliva, M., Angelovici, R., Yalovsky, S., and Ohad, N. (2004). Detection of protein-protein interactions in plants using bimolecular fluorescence complementation. *Plant J.* 40, 419–427.
23. Jurgens, G. (2005). Cytokinesis in higher plants. *Annu. Rev. Plant Biol.* 56, 281–299.
24. Otegui, M.S., Verbrugghe, K.J., and Skop, A.R. (2005). Midbodies and phragmoplasts: Analogous structures involved in cytokinesis. *Trends Cell Biol.* 15, 404–413.
25. Walther, T.C., Pickersgill, H.S., Cordes, V.C., Goldberg, M.W., Allen, T.D., Mattaj, I.W., and Fornerod, M. (2002). The cytoplasmic filaments of the nuclear pore complex are dispensable for selective nuclear protein import. *J. Cell Biol.* 158, 63–77.
26. Bischoff, F.R., Krebber, H., Kempf, T., Hermes, I., and Ponstingl, H. (1995). Human RanGTPase-activating protein RanGAP1 is a homologue of yeast Rna1p involved in mRNA processing and transport. *Proc. Natl. Acad. Sci. USA* 92, 1749–1753.
27. Haraguchi, T., Koujin, T., Hayakawa, T., Kaneda, T., Tsutsumi, C., Imamoto, N., Akazawa, C., Sukegawa, J., Yoneda, Y., and Hiraoka, Y. (2000). Live fluorescence imaging reveals early recruitment of emerin, LBR, RanBP2, and Nup153 to reforming functional nuclear envelopes. *J. Cell Sci.* 113, 779–794.
28. Ishikawa, H., and Evans, M.L. (1995). Specialized zones of development in roots. *Plant Physiol.* 109, 725–727.
29. Lincoln, C., Britton, J.H., and Estelle, M. (1990). Growth and development of the *axr1* mutants of Arabidopsis. *Plant Cell* 2, 1071–1080.
30. Mans, B.J., Anantharaman, V., Aravind, L., and Koonin, E.V. (2004). Comparative genomics, evolution and origins of the nuclear envelope and nuclear pore complex. *Cell Cycle* 3, 1612–1637.
31. Baptiste, E., Charlebois, R.L., MacLeod, D., and Brochier, C. (2005). The two tempos of nuclear pore complex evolution: Highly adapting proteins in an ancient frozen structure. *Genome Biol.* 6, R85.

#### Accession Numbers

The GenBank accession numbers for full-length cDNA sequences are BT003145 (WIP1), AY735734 (WIP2a), AY735735 (WIP2b), AY045697 (WIP3).